Multiphonon relaxation in YVO$_4$ single crystals

F. S. Ermeneux

Laboratoire de Physico-Chimie des Matériaux Luminescents, UMR 5620 CNRS, Université de Lyon I, 69622 Villeurbanne, France
and Department of Physics, Montana State University, Bozeman, Montana 59715

C. Goutaudier

Laboratoire de Physico-Chimie des Matériaux Luminescents, UMR 5620 CNRS, Université de Lyon I, 69622 Villeurbanne, France

R. Moncorgé

Laboratoire de Physico-Chimie des Matériaux Luminescents, UMR 5620 CNRS, Université de Lyon I, 69622 Villeurbanne, France
and Centre Interdisciplinaire de Recherche Ions Lasers, UMR 6637 CEA-CNRS-ISMRA, Université de Caen, 14050 Caen, France

Y. Sun and R. L. Cone

Department of Physics, Montana State University, Bozeman, Montana 59715

E. Zannoni and E. Cavalli

Dipartimento di Chimica Generale ed Inorganica, Chimica Analitica, Chimica Fisica, Università di Parma, 43100 Parma, Italy

M. Bettinelli

Dipartimento Scientifico e Tecnologico, Università di Verona, 37134 Verona, Italy
(Received 5 April 1999; revised manuscript received 16 July 1999)

Multiphonon relaxation rates were measured for 13 different energy levels of various rare-earth ions in YVO$_4$ single crystals at 77 K. Dependence of the multiphonon relaxation rate on the energy gap that separates each emitting multiplet from the one lying just below it was investigated over the range from 980 to 5200 cm^{-1}. A significant change in gap dependence was observed for energy gaps smaller than about 2500 cm^{-1}, in agreement with previous observations and with theoretical investigations. An extreme nonradiative transition rate of 1.1×10^{11} s^{-1} ($\tau = 9$ ps), corresponding to a 980 cm^{-1} energy gap, was deduced from homogeneous absorption linewidth measurements at 1.5 K.

I. INTRODUCTION

Multiphonon relaxation (MR) of rare-earth ions in glasses and crystals following optical excitation was extensively explored in the 1960s and 1970s as illustrated in Refs. 1–4. The high level of recent interest may be attributed both to the role of MR in analyzing the efficiency of recently developed solid-state laser systems and to new developments, including observation of saturation of the phonon modes at strong excitation densities with consequent improvement of the fluorescence quantum efficiency of some rare earth energy levels,[5,6] the availability of tunable short pulse laser sources at infrared wavelengths for direct measurement of very short relaxation times,[7,8] and the appearance of more complete theoretical models.[9–11]

Our attention has been concentrated recently on the growth and the optical properties of Nd^{3+}-doped YVO$_4$ single crystals,[12,13] which have proved to be among the most important diode-pumped laser materials in terms of laser threshold and laser efficiency.[14] The optical properties of YVO$_4$ doped with Er^{3+} (Refs. 15 and 16) and Tm^{3+} (Refs. 17 and 18) also have been studied to gain more insight into the electron-phonon coupling in this host matrix and to evaluate their laser potential at various wavelengths. The general characterization of MR in YVO$_4$ is the focus of the present paper.

Aspects of MR for a number of energy levels in YVO$_4$ had been studied in the past;[19,20] however, dispersion of the data points obtained for energy gaps ranging between 2200 and 3500 cm^{-1} was too great to obtain a clear exponential dependence of the measured MR rates using the well-known energy gap law. The temperature dependence of the MR rates of various rare earth levels in YVO$_4$, however, was fitted well by existing models.

To analyze these MR rates both more precisely and for a wider range of energy gaps in YVO$_4$, new fluorescence lifetime measurements were performed at low temperature (77 K) on a variety of Nd^{3+}-, Er^{3+}-, Ho^{3+}-, Eu^{3+}-, or Tm^{3+}-doped YVO$_4$ samples. The MR rates were determined either directly from the measured lifetimes in the case of small energy gaps or, when necessary, in the case of intermediate and large energy gaps, by subtracting out the radiative transition rates obtained from analysis of absorption data with the Judd-Ofelt formalism.[21,22]

A brief review of MR theories is presented in Sec. II. Section III is dedicated to description of the spectroscopic and lifetime measurements. The deduced MR rates are analyzed in Sec. IV, and conclusions stated in Sec. V.

II. THEORETICAL BACKGROUND

Different expressions for the MR probability and its temperature dependence can be found in the literature. The aim

of this section is to present the main approaches and the expressions which we have considered to analyze our own data.

Within the crystal-field approximation, the Hamiltonian of the system consisting of a rare earth dopant ion and its crystal environment can be written as

$$H = H_e + H_L + H_{eL}, \qquad (1)$$

where H_e, H_L, and H_{eL} stand for the Hamiltonian terms for the isolated impurity ion, the host lattice vibrations, and the electron-phonon interaction, respectively. Assuming small displacements u of the lattice ions about their equilibrium positions, H_{eL} can be expanded in a Taylor series, and for rare-earth ions with weak coupling to the lattice, it is reasonable to use the scalar form:[23]

$$H_{eL} = V^{(0)} + V^{(1)}u + V^{(2)}u^2 + \cdots + V^{(n)}u^n + \cdots, \qquad (2)$$

where $V^{(0)}$ and $V^{(n)} = [(\partial H_{eL}/\partial r^n)_{r=R}/n!]$ only depend on the electron coordinates.

There exist then several methods to account for MR by n-phonon nonradiative transitions.

The first approach[23–27] shows that the linear term $V^{(1)}u$ in H_{eL} can generate an n-phonon nonradiative transition. This linear mechanism of MR occurs when there is a non-zero Huang-Rhys electron-phonon coupling factor[28] and when first-order perturbation theory is used. With this approach, the dependence of the MR rate on the energy gap obeys the classic exponential energy-gap law:[4]

$$W_{nr} = C \exp[-\alpha \Delta E], \qquad (3)$$

where ΔE is the energy gap to the next lower level, C and α are constants which are characteristic of the particular host. The parameter α depends on the Huang-Rhys factor S, the phonon occupation number $\bar{n}$ at temperature T, and the number of phonons N involved to bridge the energy gap ΔE. It has to be noted that several authors prefer to use the modified expression

$$W_{nr} = C \exp[-\alpha(\Delta E - \varepsilon)] \qquad (4)$$

in which the C electronic factor does not depend so strongly on the nature of the host as in the previous expression and in which the energy gap has been reduced by some energy $\varepsilon = 2\hbar\omega_m$ (Ref. 29) or $2.6\hbar\omega_m$,[24] $\hbar\omega_m$ being the energy of the promoting phonon mode.

In the second approach[9–11] using the nonlinear mechanism, a zero electron-phonon Huang-Rhys coupling factor is assumed, and the first nonvanishing contribution to the n-phonon process arises from the $V^n u^n$ term of Eq. (2).

Within the framework of this second approach, treating the nth order nonlinear term of Eq. (2) directly as a perturbation, one can derive again the classical energy-gap law.[19] However, the experimentally measured MR rates do not always follow this law in a very wide range of ΔE values. Moreover, the α parameter only depends on the host material, no distinction can be made between the different types of active ions and no information concerning the nature (selection rules between multiplets) of the MR transitions is appearing.

So, a more elaborate treatment of this n-phonon nonlinear relaxation mechanism based on the crystal-field point charge

model approximation and including metal-ligands covalency effects as a correction was proposed recently[9–11] and resulted in a MR probability of the form:

$$W = \sum_{k=2,4,6} W_k^{pc}(1 + \bar{C}), \qquad (5)$$

with

$$W_k^{pc} = \frac{1}{137(2J+1)(2J'+1)} E_k(n) \langle LSJ \| U^{(k)} \| L'S'J' \rangle^2. \qquad (6)$$

In these expressions, $\bar{C}$ is the correction for the covalency effects, "pc" stands for "point charge" and the $E_k(n)$, which can be expressed in terms of crystal field and dynamic lattice parameters, are the intensity parameters for the n-phonon transitions. These intensity parameters are similar to the Ω_t parameters of the Judd-Ofelt formalism. The reduced matrix elements of the unit tensor operators $U^{(k)}$ of rank (k) are the same as the ones used for the calculation of the radiative spontaneous emission probabilities. According to this theory, the dependence of the MR rate on the energy gap is not a single exponential. On a logarithmic scale, a change of slope is found when the number of phonons involved exceeds 4, and such an effect is even more pronounced when the covalency between the $4f$ electrons and the ligands is considered.[10]

When considering the temperature dependence of the MR rates, a more complicated expression is obtained by considering the linear rather than the nonlinear mechanism;[4,19,23] however, both cases reduce to the same expression for small values of S and for temperatures that are not too high. When the transition is made by phonons of different energies

$$\sum_i p_i \hbar\omega_i = \Delta E \qquad (7)$$

the temperature dependence of the MR rate takes the form:

$$W(p) = W(T=0) \prod_i (n_i+1)^{p_i}, \quad \text{with} \quad \sum_i p_i = p, \qquad (8)$$

where p is the total number of emitted phonons, p_i is the number of phonons emitted with the energy $\hbar\omega_i$, and n_i is the Bose-Einstein occupation probability

$$n_i = \left[\exp\left(\frac{\hbar\omega_i}{k_B T}\right) - 1 \right]^{-1}. \qquad (9)$$

This model is known as the stimulated phonon emission model.[4]

This temperature dependence has been verified in many systems, such as those previously reported in Refs. 2, 4, 19, and 20, and the results all showed good agreement when the model used a sum of phonons of different energies and the energy of each phonon was that of a peak in the phonon density of states.

III. SPECTROSCOPIC AND LIFETIME MEASUREMENTS

Analysis of lifetime measurements depends on the relative importance of the radiative and nonradiative transition

rates. For the case of small energy gaps, where W_{nr} $\gg (\tau_r)^{-1}$ and thus $W_{nr} \approx (\tau_f)^{-1}$, the MR transition rates could be directly determined from the measured fluorescence lifetimes. In other cases, the MR transition rates were determined by subtracting the calculated radiative transition rates $(\tau_r)^{-1}$ derived by analyzing the absorption data using the JO formalism from the experimental $(\tau_f)^{-1}$ values:

$$W_{nr} = (\tau_f)^{-1} - (\tau_r)^{-1}. \qquad (10)$$

The energy-gap law given by Eq. (5) only applies in principle at low temperature, but it is well known that lifetimes do not vary much below about 100 K. In the following analysis, we shall use fluorescence lifetime data obtained at 77 K; when only room temperature (RT) data are available, we shall extrapolate the MR rates to low temperature from those obtained at room temperature by using the stimulated phonon emission model mentioned above, by writing:

$$W_{nr}(\text{LT}) = \frac{W_{nr}(\text{RT})}{\Pi_i (n_i + 1)^{p_i}}, \quad \text{with}$$

$$W_{nr}(\text{RT}) = [\tau_f(\text{RT})]^{-1} - (\tau_r)^{-1}, \qquad (11)$$

where RT denotes room temperature. For this extrapolation, the minimum number of phonons necessary to bridge the energy gap was used, and the energy of each phonon was chosen to be that of a major peak in the phonon density of states. The low-temperature fluorescence lifetime then could be directly deduced from the low-temperature nonradiative rate

$$\tau_f(\text{LT}) = [W_{nr}(\text{LT}) + (\tau_r^{-1})]^{-1}, \qquad (12)$$

where LT denotes low temperature. The somewhat arbitrary choice of phonon energies could lead to uncertainty in the calculation of the low temperature MR rates. We found, however, that this uncertainty was negligibly small.

We also used a very lightly Nd^{3+}-doped sample (0.05%) to make a very precise absorption linewidth measurement at very low temperature for the particular optical transition $^4I_{9/2}(Z1)$-$^4F_{5/2}(S1)$. The measured homogeneous linewidth of this transition reflects the very short relaxation time and very high nonradiative rate of the transition. This measurement allowed adding a further data point for the very small energy gaps.

A. Radiative lifetime estimations

As mentioned previously, the radiative lifetimes of the energy levels of interest were calculated, when necessary, using the Judd-Ofelt Ω_2, Ω_4, and Ω_6 parameters derived either from polarized absorption spectra recorded at room temperature in the visible or in the infrared or from literature data. This procedure was performed for the cases of 3.4% Er^{3+}:YVO$_4$,[15] 0.87% Tm^{3+}:YVO$_4$,[17] and 0.58% Nd^{3+}:YVO$_4$ (Ref. 30) single crystals, and the results are reported in Table 1. The absorption spectra were polarization averaged before analysis by using an average refractive index $n = 2/3 n_\sigma + 1/3 n_\pi$ with the values $n_\sigma = 1.94$ and $n_\pi = 2.14$.

B. Fluorescence lifetimes

Measurements were performed on samples with less than 1 at. % doping and at $T = 77$ K as well as at room temperature to complete or confirm the data of the literature. We thus studied the fluorescence decays of several energy levels of crystals doped by 0.58% Nd^{3+}, 0.1% Er^{3+}, 0.4% Tm^{3+}, <1% Ho^{3+}, and <1% Eu^{3+} ions. These crystals were grown as previously described.[12,15,17]

The samples were excited with a pulsed Raman-shifted Quantel dye laser (10 Hz repetition rate, 10 ns pulse duration). The specific fluorescence was selected using a Jobin-Yvon HRS1 monochromator equipped with a 600 groove/mm grating blazed at 1500 nm for investigations in the infrared domain and a 1200 groove/mm grating blazed at 500 nm for investigations in the visible. The fluorescence signals were detected either by a fast (0.5 μs) nitrogen cooled North Coast germanium photodiode for the infrared or by a Hamamatsu R1477 photomultiplier for the visible, and the signals were analyzed using a Lecroy 9400 digital oscilloscope coupled to a PC computer.

Special attention was addressed for avoiding energy transfer and reabsorption (or radiative trapping) problems, not only by working with low concentrated samples but also, for example, by selectively imaging the fluorescence spot produced by the laser onto the entrance slit of the monochromator. However, as we shall see, some uncertainties still remained, arising from experimental errors, radiative trapping but also from the Judd-Ofelt (JO) formalism in the case of the fluorescences coming from the Er^{3+} $^4I_{13/2}$, and Nd^{3+} $^4F_{3/2}$ energy levels more particularly, but also from the Tm^{3+} $^3F_4$. We report in Table I the lifetimes of several excited states for YVO$_4$ doped with a series of lanthanide ions.

Erbium

The $^4I_{13/2}$, $^4I_{11/2}$, $^4F_{9/2}$, and $^4S_{3/2}$ fluorescence lifetimes of Er^{3+} in YVO$_4$ were measured at room temperature as well as at $T = 77$ K by directly exciting each of the emitting levels (except for $^4S_{3/2}$ for which we excited the $^2H_{11/2}$ level located just above it) and by recording the fluorescence at λ = 1550, 1000, 1140, and 858 nm associated with the $^4I_{13/2}$ $\rightarrow ^4I_{15/2}$, $^4I_{11/2} \rightarrow ^4I_{15/2}$, $^4F_{9/2} \rightarrow ^4I_{13/2}$ and $^4S_{3/2} \rightarrow ^4I_{13/2}$ transitions, respectively.

The 77 K value of the $^4I_{13/2}$ lifetime with a value of 2.5 ms was found to be slightly longer than the calculated radiative lifetime of 2.45 ms.

Holmium

The $^5F_5$, $^5S_2$-$^5F_4$, and $^5F_3$ fluorescence lifetimes of the Ho^{3+} ion in YVO$_4$ were measured again at room temperature and 77 K. The $^5F_3$ and $^5S_2$-$^5F_4$ lifetimes were obtained by exciting the $^5F_3$ level and by recording the fluorescence at λ = 840 nm and λ = 544 nm associated with the $^5F_3 \rightarrow ^5I_6$ and $^5S_2$-$^5F_4 \rightarrow ^5I_8$ transitions, respectively. The $^5F_5$ fluorescence lifetime was obtained after direct excitation and by recording the fluorescence associated with the $^5F_5 \rightarrow ^5I_8$ transition at λ = 660 nm. The $^5F_3$ lifetime was too short (τ < 0.05 μs) to be measured accurately.

TABLE I. Fluorescence decay times and radiative lifetimes for various rare earth dopants and energy levels in YVO$_4$. RT denotes room temperature.

Dopant	Energy level	Radiative lifetime (Ref.) (μs)	Measured lifetime (RT) (μs)	Measured lifetime (77 K) (μs)	Previous measurements (Ref.) (μs)	ΔE (Ref.) (cm^{-1})
Nd^{3+}	$^4I_{11/2}$				RT:0.7×10^{-3} (Ref. 7) 77 K:0.75×10^{-3} [calc]	1530 (Ref. 40)
	$^4F_{3/2}$	90 (Ref. 30)	100			5050
	$^4F_{5/2}$			9×10^{-6} [1.5 K]		980.0
	$^2P_{3/2}$	4	0.10	0.13		2400
Er^{3+}	$^4I_{13/2}$	2450 (Ref. 15)	2350	2500		6500 (Ref. 15)
	$^4I_{11/2}$	1720	27	30		3600
	$^4F_{9/2}$	220	0.4	0.3		2620
	$^4S_{3/2}$	205	10	16	77 K:16 (Ref. 19)	3100
Tm^{3+}	$^3F_4$	1320 (Ref. 17)	1030	1050 [calc]		5218 (Ref. 34)
	$^3H_4$	200	135	120		4032
Ho^{3+}	$^5F_5$		0.8	1	77 K:0.7 (Ref. 18)	2020 (Ref. 41)
	$^5S_2-^5F_4$		1.7	3.5	4.2 K:17 (Ref. 19)	2854
	$^5F_3$		<0.05	<0.05		1950
Eu^{3+}	$^5D_1$		8.0	8.0	77 K:7 (Ref. 18)	1750 (Ref. 34)
	$^5D_2$		0.25	0.3		2420
	$^5D_3$		2.6	2.9 [calc]	77 K:4	2910

Europium

The $^5D_1$ and $^5D_2$ lifetimes of Eu^{3+} in YVO$_4$ were measured by directly exciting each of the levels at room temperature and 77 K and by recording the fluorescence associated with the $^5D_1\rightarrow^7F_2$ and $^5D_2\rightarrow^7F_3$ emission transitions at $\lambda=586$ nm and $\lambda=490$ nm. The $^5D_3$ lifetime was only measured at room temperature after 355 nm excitation. The Eu^{3+} ions could not be excited efficiently at such a wavelength at 77 K because of narrowing of the absorption lines, so the low temperature value had to be extrapolated using the method described above.

Thulium

In the case of Tm^{3+}-doped YVO$_4$, the $^3H_4$ fluorescence lifetime was measured at room temperature and 77 K after $^3F_2$ excitation, the $^3F_2\rightarrow^3H_4$ nonradiative relaxation being very fast, and by monitoring the $^3H_4\rightarrow^3F_4$ emission at $\lambda=1475$ nm. The $^3F_4$ lifetime was measured after direct excitation only at room temperature.

Neodymium

The $^4F_{3/2}$ fluorescence lifetime of Nd^{3+} in YVO$_4$ is subject not only to strong radiative trapping but also to stimulated emission and concentration quenching effects.[13] Our 100 μs fluorescence decay time measurement needs to be carefully interpreted. Additionally, we observed a fluorescence decay time that is slightly larger than the calculated Judd-Ofelt radiative lifetime, and we thus concluded that experimental artifacts such as radiative trapping were too important to deduce a correct MR rate.

We also give in Table I the room temperature lifetime of the $^4I_{11/2}$ level recently reported[7] and that we could not measure with our equipment. The low temperature value for the $^4I_{11/2}$ energy level was extrapolated from these room temperature data using the procedure described above.

The Nd^{3+} $^2P_{3/2}$ lifetime was measured after 355 nm excitation, at room temperature and 77 K, by monitoring the $^2P_{3/2}\rightarrow^4I_{11/2}$ emission at 476 nm.

C. Absorption linewidth measurements

In a preliminary study, we were able to show that, at $T=12$ K, the Nd^{3+} $^4I_{9/2}(Z1)$-$^4F_{5/2}(S1)$ absorption line around $\lambda=809$ nm was substantially broader than the $^4I_{9/2}(Z1)$-$^4F_{3/2}(R1)$ absorption line around $\lambda=880$ nm.[13] We thus assumed that the former could be homogeneously broadened whereas the latter would be inhomogeneously broadened as is normal at such a low temperature. To check further this assumption we used a 0.05% Nd^{3+}-doped sample and recorded these two absorption lines at even lower temperature, i.e., at $T=1.5$ K and by using a 1 MHz linewidth single mode Ti:sapphire laser. We thus confirmed that the $^4I_{9/2}(Z1)$-$^4F_{3/2}(S1)$ absorption line was inhomogeneously broadened with a Gaussian shape and a linewidth of about 1 GHz [full width at half maximum (FWHM)] whereas the $^4I_{9/2}(Z1)$-$^4F_{5/2}(S1)$ absorption line was Lorentzian with a width of 18 GHz, which is much broader.

Stimulated direct one phonon processes within the first Stark levels of the $^4F_{5/2}$ and $^4I_{9/2}$ multiplets could give some contribution to the homogeneous broadening of the $^4I_{9/2}(Z1)\rightarrow^4F_{5/2}(S1)$ transition even at such a low temperature (1.5 K);[31] however, the positions of the second Stark levels of both the $^4I_{9/2}$ and $^4F_{5/2}$ multiplets are high enough (40 cm^{-1} for $^4F_{5/2}$ and 110 cm^{-1} for $^4I_{9/2}$) and the density of available phonons sufficiently low to eliminate this possibility. The Raman contribution to the broadening is also assumed to be negligible at such a low temperature so that the
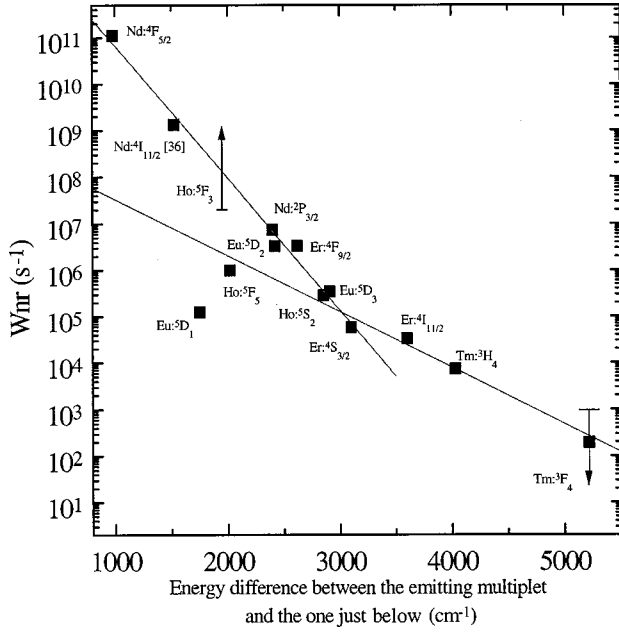
FIG. 1. Multiphonon relaxation rates of various rare earth emitting levels in YVO₄ as a function of the energy gaps between these levels and those lying just below.

observed Lorentzian broadening of the $^4I_{9/2}(Z1)$-$^4F_{5/2}(S1)$ absorption line is assigned to lifetime broadening. Consequently, the $^4F_{5/2}$ lifetime can be directly deduced from the homogeneous linewidth and the result is

$$\tau(1.5\,\text{K}) = \frac{1}{2\pi\Delta\upsilon} = 9 \text{ ps.} \qquad (13)$$

This very short value means an MR rate of about $1.1 \times 10^{11}\,\text{s}^{-1}$.

IV. DISCUSSION OF THE RESULTS

Figure 1 shows on a semilog scale all of the MR rates W_{nr} that we were able to derive from our fluorescence and radiative lifetime data [using Eqs. (10)–(12)] as a function of the energy gap ΔE between the lowest Stark level of each emitting multiplet and the highest Stark level of the multiplet lying just below it.

Because of different artifacts due to radiative trapping and stimulated emission effects[13] we did not try to report in the figure the point corresponding to the $^4F_{3/2}$ emission of Nd³⁺. Concerning the $^4I_{13/2}$ and $^3F_4$ emissions of the Er³⁺ and Tm³⁺ ions, respectively, we could consider that the discrepancies between the fluorescence and radiative lifetimes were also due to radiative trapping or to combined uncertainties of the fluorescence lifetimes, absorption spectra and rare-earth concentration measurements, as was concluded for example in Ref. 32. However, according to Ref. 33, such discrepancies could also come from the inadequacy of the JO formalism in the calculation of the radiative lifetime between two multiplets experiencing large crystal-field splittings. Following the same procedure as in Ref. 33 and using the $^4I_{13/2} \leftrightarrow {}^4I_{15/2}$ and $^3F_4 \leftrightarrow {}^3H_6$ absorption and emission data for Er³⁺ (Refs. 15 and 34) and Tm³⁺,[34,35] effective statistical weight ratios of about 1.2 and 0.8 were estimated, respec-

tively, giving corrected radiative lifetimes $\tau_R = 2.35 \times (1.2/0.87) = 3.25$ ms for Er³⁺ and $\tau_R = 1.32 \times (0.8/0.69) = 1.53$ ms for Tm³⁺. The value obtained for Er³⁺ would indicate a nonradiative probability of about 90 s⁻¹ for an energy gap of 6500 cm⁻¹. This point would not be aligned with the other points corresponding to the largest energy gaps. Moreover, this value would suggest a $^4I_{13/2}$ fluorescence quantum efficiency of less than 80%, which is rather surprising but might be possible. On the other hand, the value obtained for Tm³⁺ would result in a nonradiative probability of about 320 s⁻¹, which is only slightly higher than the value reported in Fig. 1 and still within the limits of the experimental errors. So, we chose not to report any of these points in Fig. 1.

According to Fig. 1, in agreement with the predictions of the *n*-phonon nonlinear relaxation theory, the dependence of the nonradiative rates on the energy gaps is not a single exponential. There is a change of slope for $\Delta E \approx 3000\,\text{cm}^{-1}$, which corresponds to about 3 phonons in the case of YVO₄. If the classical energy gap law was still valid, the W_{nr} values could be fitted with two exponentials depending on the ΔE values. For $\Delta E < 3000\,\text{cm}^{-1}$, the C and α parameters involved in the expression (3) would be given by

$$C = 4.8 \times 10^{13}\,\text{s}^{-1} \quad \text{and} \quad \alpha = 6.6 \times 10^{-3}\,\text{cm}$$

and for $\Delta E > 3000\,\text{cm}^{-1}$:

$$C = 4 \times 10^8\,\text{s}^{-1} \quad \text{and} \quad \alpha = 2.6 \times 10^{-3}\,\text{cm.}$$

It is to be noted first that the highest MR rate of $1.1 \times 10^{11}\,\text{s}^{-1}$ deduced from the low temperature absorption linewidth measurement reported above is associated with an energy gap between levels $^4F_{5/2}$ and $^4F_{3/2}$ of about 980 cm⁻¹, a value that is slightly larger than the highest phonon energy 950 cm⁻¹ (Ref. 19) found in the phonon and the vibronic spectra of rare-earth-doped YVO₄.

On the other hand, we also note that most of the points fit nicely with the above defined exponentials. Two data points, however, seem to be completely inconsistent. First, the $^5D_1$ (Eu³⁺) MR rate is more than three orders of magnitude smaller than it should be. This behavior has been observed before;[36,37] it is directly related to the Judd-Ofelt-based selection rules which state that for rare earth ions with even numbers of electrons, the radiative transition between $J=0$ and $J=1,3,5$ should be weak (Ref. 22). According to Eq. (6), the MR probability depends on the reduced matrix element: $\langle LSJ \| U^{(k)} \| L'S'J' \rangle$. The nonradiative transitions between multiplets are thus influenced by the same Judd-Ofelt selection rules as the radiative transitions. This is also the reason why the $^3P_1$ level of Pr³⁺ can be found to be an emitting multiplet at low temperature: the fluorescence lifetime of this $^3P_1$ energy level in Pr³⁺:YVO₄ measured at $T=2$ K was found to be 250 μs. The $^3P_1$ level is only 600 cm⁻¹ above the $^3P_0$ metastable level and its lifetime is thus far longer than would be expected in the case of a single- or multiphonon nonradiative transition.[38]

The more than one order of magnitude too weak MR probability for Ho³⁺:$^5F_5$ could not be explained.

At small energy gaps (980–3000 cm⁻¹), two other reasons for slight variations from the energy gap law can be

pointed out. First, it has been shown[20] that for less than 2-phonon transitions, the existence of vibronic peaks can have a significant influence on the MR, and a small difference of 8 cm^{-1} between two gaps can lead to a factor of more than fivefold difference between the two associated MR rates. However, this effect seems to be inefficient for more than 2-phonon transitions. Second, deviations from the energy gap law are directly associated with Eq. (6), which shows that, considering the corrected point charge model, the MR probability depends on the reduced matrix element $\langle LSJ \| U^{(k)} \| L'S'J' \rangle$ of the unit tensor operator $U(k)$ of rank (k) for the transition within the $4f$ electronic configuration. This directly implies more or less important deviations of MR rates from a single exponential law from one transition to another.

At higher energy gaps ($\Delta E > 3000 \, \text{cm}^{-1}$) we can see that the influence of radiative lifetimes on the calculation of MR becomes important. The Nd^{3+} $^4F_{3/2}$, Tm^{3+} $^3F_4$, and Er^{3+} $^4I_{13/2}$ levels have a lifetime close to the radiative one, and the uncertainties associated with both the Judd-Ofelt theory and the lifetime measurements may lead to very significant uncertainties on the MR rate calculations when the energy gap is larger than 4500 cm^{-1}. Thus, the data for Nd^{3+} $^4F_{3/2}$, Tm^{3+} $^3F_4$, and Er^{3+} $^4I_{13/2}$ need to be carefully interpreted.

The strong change in slope observed for energy gaps around 3000 cm^{-1} is in good agreement with the observations reported in Refs. 9, 10, and 39 and can be interpreted according to the point charge theory by including a correction taking into account the covalency effects on the bonding of $4f$ electrons and the lattice ions (Sec. II).

V. CONCLUSIONS

MR rates were studied for a series of rare-earth ion energy levels, and fits to theoretical expressions resulted in an exponential functional form. A strong reduction of slope was observed around 3000 cm^{-1}, which can be interpreted on the basis of a corrected point charge model. A new approach was used to measure the ultrafast MR rates of the $^4F_{5/2}(S1)$ energy level of Nd^{3+}, and an extremely short relaxation time of 9 ps has been determined for the lifetime. This confirms the order of magnitude of the Nd^{3+} $^4I_{11/2}$ lifetime measured previously in YVO$_4$.[7]

Further studies on rare-earth-doped oxide crystals such as YAG, YVO$_4$, or Y$_2$O$_3$ will show that a few rare earth energy levels have energy gaps slightly larger than the maximum phonon energy of the matrix and have lifetime limited homogeneous absorption linewidths. For example, a lifetime of 3.4 ps has already been measured at 1.5 K for the $^4F_{5/2}$ level of a 0.0013% Nd^{3+}:YAG crystal. To use this approach, very lightly doped crystals are necessary to limit the inhomogeneous linewidth of the absorption transitions.

[1] M. J. Weber, Phys. Rev. **156**, 231 (1967).

[2] W. D. Partlow and H. W. Moos, Phys. Rev. **157**, 252 (1967).

[3] M. J. Weber, Phys. Rev. **157**, 262 (1967).

[4] L. A. Riseberg and H. W. Moos, Phys. Rev. **174**, 429 (1968).

[5] F. Auzel and F. Pellé, Opt. Mater. **8**, 15 (1997).

[6] F. Auzel and F. Pellé, C. R. Acad. Sci., Ser. IIb: Mec., Phys., Chim., Astron. **322**, 835 (1996).

[7] C. Bibeau, S. A. Payne, and H. T. Powell, J. Opt. Soc. Am. B **12**, 1981 (1995).

[8] C. Bibeau and S. A. Payne, in *Advanced Solid State Lasers*, edited by W. R. Bosenberg and M. M. Fejer (Optical Society of America, Washington, D.C., 1998), pp. 433–436.

[9] Y. V. Orlovski, R. J. Reeves, R. C. Powell, T. T. Basiev, and K. K. Pukhov, Phys. Rev. B **49**, 3821 (1994).

[10] Y. V. Orlovski, K. K. Pukhov, T. T. Basiev, and T. Tsuboi, Opt. Mater. **4**, 583 (1995).

[11] K. K. Pukhov and V. P. Sakun, in *Physics and Spectroscopy of Laser Crystals*, edited by A. A. Kaminski (Nauka, Moscow, 1986), p. 150.

[12] C. Goutaudier, F. S. Ermeneux, M. T. Cohen-Adad, R. Moncorgé, M. Bettinelli, and E. Cavalli, Mater. Res. Bull. **33**, 1457 (1998).

[13] F. S. Ermeneux, C. Goutaudier, R. Moncorgé, M. T. Cohen-Adad, M. Bettinelli, and E. Cavalli, Opt. Mater. **13**, 193 (1999).

[14] T. S. Lomheim and L. G. DeShazer, J. Appl. Phys. **49**, 5517 (1978); see also L. G. DeShazer, Laser Focus World **30**(2), 88 (1994).

[15] P. Kabro, J. A. Capobianco, F. S. Ermeneux, R. Moncorgé, M. Bettinelli, and E. Cavalli, Chem. Phys. **214**, 329 (1997).

[16] P. Kabro, J. A. Capobianco, F. S. Ermeneux, R. Moncorgé, M. Bettinelli, and E. Cavalli, J. Appl. Phys. **82**, 3983 (1997).

[17] F. S. Ermeneux, C. Goutaudier, R. Moncorgé, M. T. Cohen-Adad, M. Bettinelli, and E. Cavalli, Opt. Mater. **8**, 83 (1997).

[18] M. Bettinelli, F. S. Ermeneux, R. Moncorgé, and E. Cavalli, J. Phys.: Condens. Matter **10**, 8207 (1998).

[19] E. D. Reed and H. W. Moos, Phys. Rev. B **8**, 980 (1973).

[20] E. D. Reed and H. W. Moos, Phys. Rev. B **8**, 988 (1973).

[21] B. R. Judd, Phys. Rev. **127**, 750 (1962).

[22] G. S. Ofelt, J. Chem. Phys. **37**, 511 (1962).

[23] B. Henderson and G. F. Imbusch, *Optical Spectroscopy of Inorganic Solids* (Oxford, Clarendon, 1989).

[24] F. Auzel, in *Luminescence of Inorganic Solids*, edited by B. DiBartolo (Plenum, New York, 1978), p. 67.

[25] T. Miyakawa and D. L. Dexter, Phys. Rev. B **1**, 2961 (1970).

[26] R. Englman, *Non Radiative Decay of Ions and Molecules in Solids* (North-Holland, Amsterdam, 1979).

[27] E. Gutsche, Phys. Status Solidi B **109**, 583 (1982).

[28] K. Huang and A. Rhys, Proc. R. Soc. London, Ser. A **204**, 406 (1950).

[29] J. M. F. van Dijk and M. F. H. Schuurmans, J. Chem. Phys. **78**, 5317 (1983).

[30] O. Guillot-Noël, Ph.D. thesis, Université P. et M. Curie, Paris VI, 1998; the values $\Omega_2 = 12 \times 10^{-20}$ cm^2, $\Omega_4 = 6.3 \times 10^{-20}$ cm^2, and $\Omega_6 = 10.1 \times 10^{-20}$ cm^2 for 0.58% Nd:YVO$_4$ are reported (measured dopant concentration)

[31] G. M. Wang, R. W. Equall, R. L. Cone, M. J. M. Leask, K. W. Godfrey, and F. R. Wondre, Opt. Lett. **21**, 818 (1996).

[32] S. A. Payne, L. L. Chase, L. K. Smith, W. L. Kway, and W. F. Krupke, IEEE J. Quantum Electron. **28**, 2619 (1992).

[33] F. Auzel, D. Meichenin, A. Mendorioz, R. Balda, and J. Fernan-

dez, J. Lumin. **72-74**, 152 (1997).

[34] A. A. Kaminskii, *Crystalline Lasers: Physical Processes* (CRC Press, Boca Raton, FL, 1996).

[35] F. S. Ermeneux, Ph.D. thesis, Université Claude Bernard, Lyon 1, 1999.

[36] E. Nardi and S. Yatsiv, J. Chem. Phys. **37**, 2333 (1962).

[37] M. J. Weber, in *Optical Properties of Ions in Crystals*, edited by H. M. Crosswhite and H. W. Moos (Interscience, New York, 1967), pp. 467–484.

[38] G. H. Dieke and R. Sarup, J. Chem. Phys. **29**, 741 (1958).

[39] T. T. Basiev, A. Y. Dergachev, Y. V. Orlovski, and A. M. Prokhorov, J. Lumin. **53**, 19 (1992).

[40] P. A. Tanner and N. Edelstein, Chem. Phys. Lett. **152**, 140 (1988).

[41] M. Enderle, B. Pilawa, W. Schaphof, and H. G. Kahle, J. Phys.: Condens. Matter **2**, 4685 (1990).